

On the scaling of the damping time for resonantly damped oscillations in coronal loops

Iñigo Arregui¹, José Luis Ballester¹, Marcel Goossens^{2,1}

ABSTRACT

There is not as yet full agreement on the mechanism that causes the rapid damping of the oscillations observed by TRACE in coronal loops. It has been suggested that the variation of the observed values of the damping time as function of the corresponding observed values of the period contains information on the possible damping mechanism. The aim of this Letter is to show that, for resonant absorption, this is definitely not the case unless detailed a priori information on the individual loops is available.

Subject headings: MHD — Sun: corona — Sun: magnetic fields — waves

1. Introduction

Transverse oscillations in coronal loops have been detected in observations made with the EUV telescope on board of the Transition Region and Coronal Explorer (TRACE) in 1999 by Aschwanden et al. (1999) and Nakariakov et al. (1999). Since then the detection of these oscillations has been confirmed and in addition damped oscillations have been observed in hot coronal loops by the SUMER instrument on board SOHO (Wang et al. 2002; Kliem et al. 2002). The TRACE oscillations have periods of the order of $\simeq 2 - 10$ minutes and comparatively short damping times of the order of $\simeq 3 - 20$ minutes. There is general consensus that these oscillations are fast standing kink mode oscillations. However, there is still debate about the mechanism that causes the observed fast damping. Different mechanisms have been suggested: phase mixing (Ofman & Aschwanden 2002), resonant absorption (Hollweg & Yang 1988; Goossens et al. 2002; Ruderman & Roberts 2002), lateral and foot-point wave leakage (Smith et al. 1997; De Pontieu et al. 2001), drag due

¹Departament de Física, Universitat de les Illes Balears, E-07122 Palma de Mallorca, Spain. Email: inigo.arregui@uib.es, dfsjlb0@uib.es

²Centre Plasma Astrophysics, Katholieke Universiteit Leuven, Leuven, B-3001, Belgium. Email: marcel.goossens@wis.kuleuven.be

to the ambient plasma (Chen & Schuck 2007). In order to discriminate between different damping mechanisms Ofman & Aschwanden (2002) suggested to study how the observed damping times vary as a function of the corresponding observed periods. In particular Ofman & Aschwanden (2002) claimed that the observed values are compatible with phase mixing if the damping time increases with period T as $T^{4/3}$ and with resonant absorption if it increases as T . The aim of the present Letter is to show that random observations of oscillation events in coronal loops are very unlikely to produce any particular relation between damping times and periods whatever the actual mechanism is that causes the damping. In particular we focus on resonant absorption and use synthetic data for periods and damping times to show that various samples of pairs of periods and damping times can lead to various and widely different scaling laws.

2. Analytical theory

The suggestion that the damping time increases linearly with period, $\tau_d \sim T$, was triggered by analytical asymptotic expressions for the damping of the quasi-mode given by e.g. Goossens et al. (1992), Ruderman & Roberts (2002), Goossens et al. (2002) (see reviews Goossens et al. 2006 and Goossens 2008). These asymptotic expressions are derived in the approximation that the non-uniform layer is thin. This is the so-called thin boundary (TB) approximation. Jump conditions are used to connect the solution over the ideal singularity and to avoid solving the non-ideal MHD wave equations (see e.g. Sakurai et al. 1991; Goossens et al. 1995). The asymptotic expression for the damping time in the TB approximation is

$$\frac{\tau_d}{T} = F \frac{R}{l} \frac{\zeta + 1}{\zeta - 1}, \quad (1)$$

where $\zeta = \rho_i/\rho_e$ is the density contrast, ρ_i and ρ_e the constant internal and external densities, l the thickness of the non-uniform layer defined in $[R - l/2, R + l/2]$, and R the mean radius. F is a parameter that depends on the variation of density in the transitional layer. For a linear variation $F = 4/\pi^2$ (Hollweg & Yang 1988; Goossens et al. 1992), for a sinusoidal variation $F = 2/\pi$ (Ruderman & Roberts 2002). In what follows we shall use the version with $F = 2/\pi$.

Equation (1) might be considered to be an invitation for predicting a linear variation of damping time with period. However, the crucial point for this prediction to make sense is that the remaining quantities in equation (1) are constants; i.e. all the oscillations events under considerations have to occur in loops with the same density contrast ζ and the same

radial inhomogeneity l/R . When applied to a collection of oscillating loops on which no prior information on their structure is available equation (1) does not allow any prediction. A naive use of equation (1) indicates that for a given period T the damping times can differ by f.e. a factor 50/3 for the combinations $\zeta = 1.5, l/R = 0.1$ and $\zeta = 5, l/R = 0.5$.

This is indeed a naive use of equation (1) since T is a function of ζ also. In order to make that clear we use results from the thin tube (TT) or long wave-length approximation for the period T . Our starting point is the well-known expression for the square of the frequency of the kink mode in a cylinder with a uniform and straight magnetic field along the z -axis (see e.g. Edwin & Roberts 1983)

$$\omega^2 = \omega_k^2 = \frac{\rho_i \omega_{A,i}^2 + \rho_e \omega_{A,e}^2}{\rho_i + \rho_e}, \quad (2)$$

where $\omega_A = k_z v_A$ is the local Alfvén frequency and $v_A = B/\sqrt{\mu\rho}$ the local Alfvén velocity (the subscripts “i” and “e” refer to internal and external, respectively). Now we note that for the fundamental mode $k_z = \pi/L$, with L the length of the loop, and we convert frequencies to periods and rewrite equation (2) as

$$\frac{T}{\tau_{A,i}} = \sqrt{2} A(\zeta), \quad (3)$$

where $\tau_{A,i} = L/v_{A,i}$ is the internal Alfvén travel time and the function $A(\zeta)$ is defined as

$$A(\zeta) = \left(\frac{\zeta + 1}{\zeta} \right)^{1/2}. \quad (4)$$

It is convenient to adopt a reference loop with magnetic field strength B_0 , length L_0 , and internal density ρ_{i0} . This reference loop allows us to consider loops of different dimensions and to introduce the normalized period T^* defined as

$$T^* = \frac{T}{(\sqrt{2})\tau_{A,i0}}. \quad (5)$$

T^* can be interpreted as the period measured in the unit $\tau_{A,i0}\sqrt{2}$. With this normalized period equation (3) takes the simple form

$$T^* = a A(\zeta), \quad (6)$$

with $a = \tau_{A,i}/\tau_{A,i0}$. From equation (6) we learn that, for a given value of a , T^* varies continuously from $\sqrt{2}a$ to a when ζ is allowed to vary from 1 (no loop) to ∞ (outside vacuum).

Let us now turn back to equation (1) and rewrite it as

$$\frac{\tau_d}{\tau_{A,i}} = \frac{2\sqrt{2}}{\pi} B(\zeta) \frac{1}{l/R}, \quad (7)$$

with the function $B(\zeta)$ defined as

$$B(\zeta) = \left(\frac{\zeta+1}{\zeta-1} \right)^{1/2} \frac{\zeta+1}{\zeta-1} = A(\zeta) \frac{\zeta+1}{\zeta-1}. \quad (8)$$

In what follows we shall refer to the combination of the TB approximation to compute the damping time and the TT approximation for the period as the TTTB approximation.

In the same way as for the period it is convenient to introduce the normalized decay time τ_d^* as

$$\tau_d^* = \frac{\tau_d}{(2\sqrt{2}/\pi)\tau_{A,i0}}. \quad (9)$$

τ_d^* can be interpreted as the decay time measured in the unit $\tau_{A,i0}$ ($2\sqrt{2}/\pi$). With the use of this normalized decay time we can write equation (7) as

$$\tau_d^* = a B(\zeta) \frac{1}{l/R}, \quad (10)$$

which tells us that, for a given value of a , τ_d^* depends on ζ and l/R . The dependency on l/R is straightforward. The dependency on ζ is slightly more complicated. Basically, τ_d^* is a decreasing function of ζ varying from $+\infty$ for $\lim \zeta \rightarrow 1$ to $\frac{a}{l/R}$ for $\lim \zeta \rightarrow +\infty$. In summary, τ_d^* is a decreasing function of both l/R and ζ .

We now combine equations (6) and (10). On Figure 1 we have plotted τ_d^* versus T^* for values of ζ from 1.5 up to 10 and of l/R from 0.01 to 2. For every value of a the pairs (T^*, τ_d^*) define a vertical strip in the (T^*, τ_d^*) -plane with a maximum horizontal extent of $(\sqrt{2} - 1)a$. As a matter of fact a can take on any positive real value, but for clarity we have limited the values to $a = 1, 2, 3, 4, 5$. The inclusion of intermediate values of a , such as $a = 4/3, 5/3, 7/3$, produces vertical strips overlapping those shown on Figure 1. The iso-lines corresponding to

a constant value of ζ are vertical lines since the period is independent of the inhomogeneity length scale, in the thin tube approximation. The iso-lines corresponding to a constant value of l/R are not straight and defined by the equation

$$\tau_d^* = \frac{(T^*)^3}{2a^2 - (T^*)^2} \frac{1}{l/R} \quad \text{for } T^* \in [a, a\sqrt{2}]. \quad (11)$$

It is clear from Figure 1 that the model of resonant absorption in its most simple mathematical formulation using the TTTB approximation produces a wide variety of combinations of (T^*, τ_d^*) . Now let us see what happens when a collection of pairs (T^*, τ_d^*) is drawn from this reservoir.

3. Scaling laws: how many do we want?

The aim of this section is to show that different collections of data can be produced by the simple TTTB mathematical model of resonant absorption with each of them leading to scaling laws, $\tau_d^* / (T^*)^n = C$ (with C a function of the equilibrium parameters), with different indices, n . We use equations (6) and (10), together with the particular relation between τ_d^* and T^* for each index n , and derive those collections of data. As a first example we have plotted on Figure 2 a collection of (T^*, τ_d^*) combinations drawn from the big reservoir depicted on Figure 1. These combinations define a scaling law with index $n = -1$. It is clear that we have engineered the data presented on Figure 2 so as to fit the scaling law with such index. Actually, the engineering is relatively straightforward. We require $T^* \tau_d^* = C_s$. The left-hand side is the value of the function C for a starting configuration with $a = a_s$, $\zeta = \zeta_s$, and $l/R = (l/R)_s$. We fix a loop to start with by prescribing the values $a_s = 1$, $\zeta_s = 1.5$, and $(l/R)_s = 0.1$ and compute values of a , ζ , and l/R that satisfy the equation

$$\frac{l}{R} = \left(\frac{l}{R} \right)_s \left(\frac{a}{a_s} \right)^2 \frac{f(\zeta)}{f(\zeta_s)}; \quad f(\zeta) = A(\zeta) B(\zeta). \quad (12)$$

Likewise on Figure 2 we have also plotted a second collection of data that now define a scaling law with index $n = 2$. To obtain these data, we start from a loop with prescribed values $a_s = 1$, $\zeta_s = 5$, and $(l/R)_s = 1$ and compute values of a , ζ , and l/R that satisfy the equation

$$\frac{l}{R} = \left(\frac{l}{R} \right)_s \frac{a_s}{a} \frac{g(\zeta)}{g(\zeta_s)}; \quad g(\zeta) = \frac{B(\zeta)}{(A(\zeta))^2}. \quad (13)$$

A third collection of data, that now define a scaling law with index $n = 4/3$ is also shown in Figure 2. According to Ofman & Aschwanden (2002) this value of the index singles out

phase mixing as damping mechanism. Here it is obtained for a collection of data that are produced by the theoretical prediction for resonant absorption. We start from a loop with prescribed values $a_S = 1$, $\zeta_S = 3$, and $(l/R)_S = 0.5$ and compute values of a , ζ , and l/R that satisfy the equation

$$\frac{l}{R} = \left(\frac{l}{R} \right)_S \left(\frac{a_S}{a} \right)^{1/3} \frac{h(\zeta)}{h(\zeta_S)}; \quad h(\zeta) = \frac{B(\zeta)}{(A(\zeta))^{4/3}}. \quad (14)$$

Finally, on Figure 2 we have also plotted a collection of data that define a scaling law with the canonical value $n=1$ for the index. We start from a loop with prescribed values $a_S = 1$, $\zeta_S = 2.5$, and $(l/R)_S = 0.2$ and compute values of a , ζ , and l/R that satisfy the equation

$$\frac{l}{R} = \left(\frac{l}{R} \right)_S \frac{c(\zeta)}{c(\zeta_S)}; \quad c(\zeta) = \frac{B(\zeta)}{A(\zeta)} = \frac{\zeta + 1}{\zeta - 1}. \quad (15)$$

Note that a is absent from (15) meaning that a solution of (15) can be combined with any value of $a > 0$. An obvious solution to (15) is

$$\zeta = \zeta_S, \quad \frac{l}{R} = \left(\frac{l}{R} \right)_S, \quad a > 0. \quad (16)$$

Equation (16) defines a straight line in the (T^*, τ_d^*) -plane. Note that equation (16) is not the only solution in the (T^*, τ_d^*) -plane. Any combination (T^*, τ_d^*) that satisfies equation (15) combined with $a \in]0, \infty[$ produces the same straight line in the (T^*, τ_d^*) plane as solution (16). Since the function $c(\zeta)$ is a decreasing function of its argument, a value $\zeta > \zeta_S$ is combined with a value $l/R < (l/R)_S$ and conversely a value $\zeta < \zeta_S$ is combined with a value $l/R > (l/R)_S$.

It is clear from Figure 2 that almost any scaling law can be obtained from data produced by the simple TTTB mathematical model of resonant absorption. All the periods and damping times plotted in Figure 2 correspond to combinations of ζ and l/R , obtained from equations (12), (13), (14), and (15), that are reasonable values of these quantities in the ranges $\zeta \in [1.5, 10]$ and $l/R \in [0.016, 1.59]$. The discrete sets of values in Figure 2 arise due to the considered discrete values of a , but loops with different internal travel times, with respect to the reference loop, would give the full set of values for τ_d^* and T^* along the solid lines depicted in Figure 2.

4. Beyond the TTTB approximation

The TTTB approximation as a mathematical model for resonant absorption has its clear limitations. First, the values of the period defined by equation (6) are independent of the radius R and the inhomogeneity length scale l/R . In reality, the period is a function of the density contrast ζ , l/R , and R . As a consequence the iso-lines corresponding to a constant value of ζ in the (T^*, τ_d^*) -plane are no longer straight vertical lines. For a given value of a this dependency of the period on ζ produces additional spread on the original vertical strips. Second, the TTTB approximation is an accurate approximation as long as the damping time is sufficiently longer than the period, since this is an inherent assumption for carrying out the asymptotic analysis leading to equation (1). We can expect this equation to be inaccurate for large values of the density contrast ζ and large values of the inhomogeneity length scale l/R . Figure 3 is the twin version of Figure 1 with the values of T^* and τ_d^* now computed for fully non-uniform 1-D loops (Van Doorsselaere et al. 2004). Figure 3 is very similar in appearance to Figure 1. The differences occur where they expected to occur. The vertical strips of Figure 1 are now replaced with strips slightly oblique to the vertical axis and the largest differences appear at the short values of the damping times corresponding to the large values of the density contrast ζ and large values of the inhomogeneity length scale l/R . The basic message from both figures is the same. The model of resonant absorption produces a wide variety of combinations in the (T^*, τ_d^*) -plane. If we draw a curve defined by a given relation between T^* and τ_d^* , for instance $\tau_d^*/(T^*)^2 = C$, in this plane we can graphically determine as many points on this curve as we want. If we select the data determined in this way the result is a scaling law with index $n = 2$ as the one in Figure 2. The only difference is that now the procedure is numerical all the way.

5. Conclusion

In this Letter we have explained that scaling laws for a group of observations of oscillating loops to discriminate between different damping mechanisms are of not much use if there is no a priori information on the properties of the loops. The analytical expressions obtained by the TTTB approximation enable us to show in a straightforward and easy to follow manner that in the framework of resonant absorption collections of synthetic data can be produced that follow almost any scaling law. Then, we have backed up our findings by numerical eigenvalue computations that do not suffer from the TTTB limitations but are on their own rather less instructive.

It might be argued that nature is not as cunning as the authors of this paper and does not attempt to engineer data according to prescribed rules as those defined in these equations.

On the other hand, there is no reason why nature would want to produce coronal loops that all have the same values of ζ and l/R . So, unless there is accurate a priori information on the coronal loops available, the use of scaling laws to discriminate between different damping mechanisms is questionable, to say the least.

It is a pleasure for MG to acknowledge the warm hospitality of JLB, the friendly atmosphere of the Solar Physics Group at the UIB, and the visiting position from the UIB. MG also acknowledges the FWO-Vlaanderen for awarding him a sabbatical leave. IA and JLB acknowledge the funding provided under projects AYA2006-07637 (Spanish MEC) and PRIB-2004-10145 and PCTIB2005GC3-03 (Government of the Balearic Islands). The authors are grateful to R. Oliver, J. Terradas, and T. Van Doorsselaere for comments and suggestions.

REFERENCES

Aschwanden, M. J., Fletcher, L., Schrijver, C. J., & Alexander, D. 1999, *ApJ*, 520, 880

Chen, J. & Schuck, P. W. 2007, *Sol. Phys.*, 246, 145

De Pontieu, B., Martens, P. C. H., & Hudson, H. S. 2001, *ApJ*, 558, 859

Edwin, P. M. & Roberts, B. 1983, *Sol. Phys.*, 88, 179

Goossens, M. 2008, in *Proceedings IAU Symposium No. 247*, ed. R. Erdelyi & C. Mendoza

Goossens, M., Andries, J., & Arregui, I. 2006, *Royal Society of London Philosophical Transactions Series A*, 364, 433

Goossens, M., Andries, J., & Aschwanden, M. J. 2002, *A&A*, 394, L39

Goossens, M., Hollweg, J. V., & Sakurai, T. 1992, *Sol. Phys.*, 138, 233

Goossens, M., Ruderman, M. S., & Hollweg, J. V. 1995, *Sol. Phys.*, 157, 75

Hollweg, J. V. & Yang, G. 1988, *J. Geophys. Res.*, 93, 5423

Kliem, B., Dammasch, I. E., Curdt, W., & Wilhelm, K. 2002, *ApJ*, 568, L61

Nakariakov, V. M., Ofman, L., DeLuca, E. E., Roberts, B., & Davila, J. M. 1999, *Science*, 285, 862

Ofman, L. & Aschwanden, M. J. 2002, *ApJ*, 576, L153

Ruderman, M. S. & Roberts, B. 2002, *ApJ*, 577, 475

Sakurai, T., Goossens, M., & Hollweg, J. V. 1991, *Sol. Phys.*, 133, 227

Smith, J. M., Roberts, B., & Oliver, R. 1997, *A&A*, 317, 752

Van Doorselaere, T., Andries, J., Poedts, S., & Goossens, M. 2004, *ApJ*, 606, 1223

Wang, T., Solanki, S. K., Curdt, W., Innes, D. E., & Dammasch, I. E. 2002, *ApJ*, 574, L101

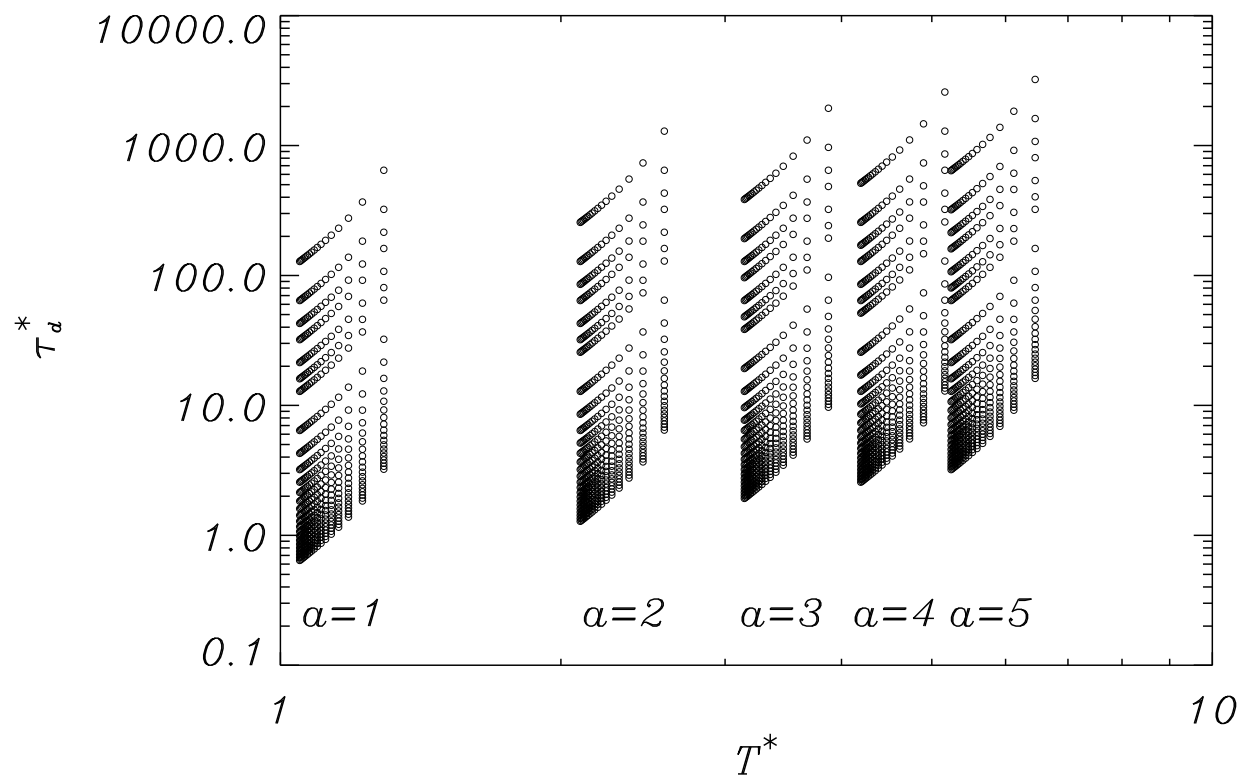


Fig. 1.— Normalized damping time as a function of the normalized period for discrete values of $\zeta \in [1.5, 10]$ and $l/R \in [0.01, 2]$, and five values of a .

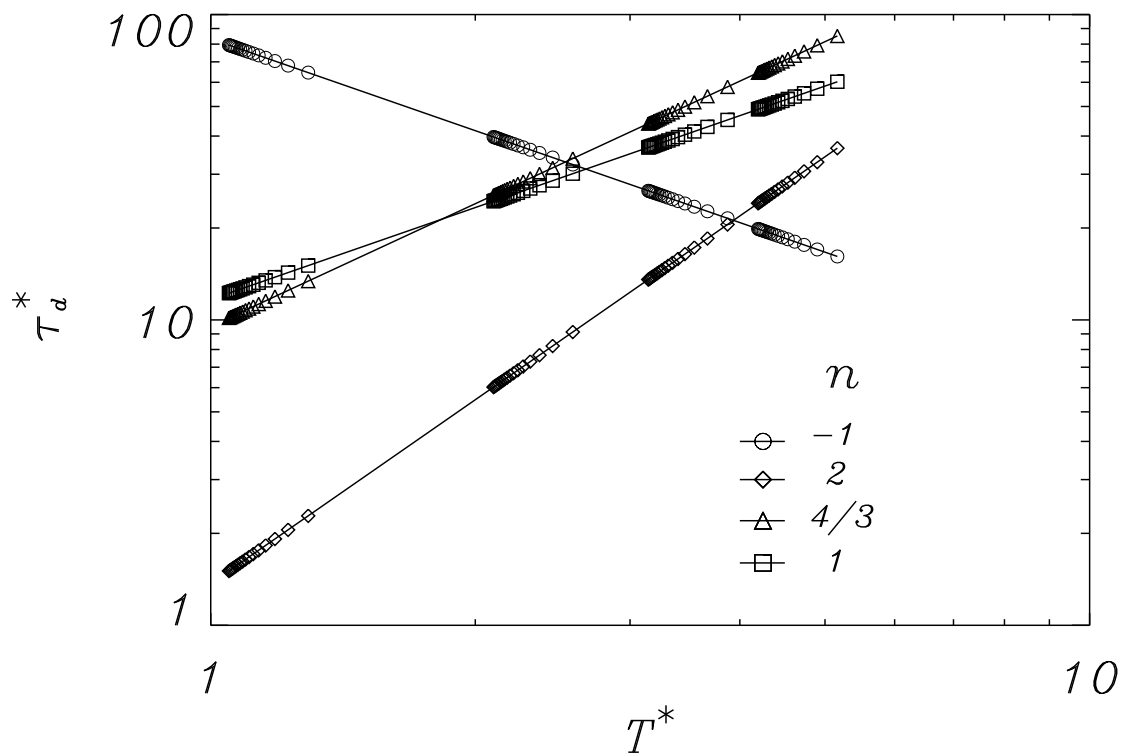


Fig. 2.— Four synthetic scaling laws corresponding to $n = -1, 4/3, 1, 2$, and values of a , from left to right, $a = 1, 2, 3, 4$.

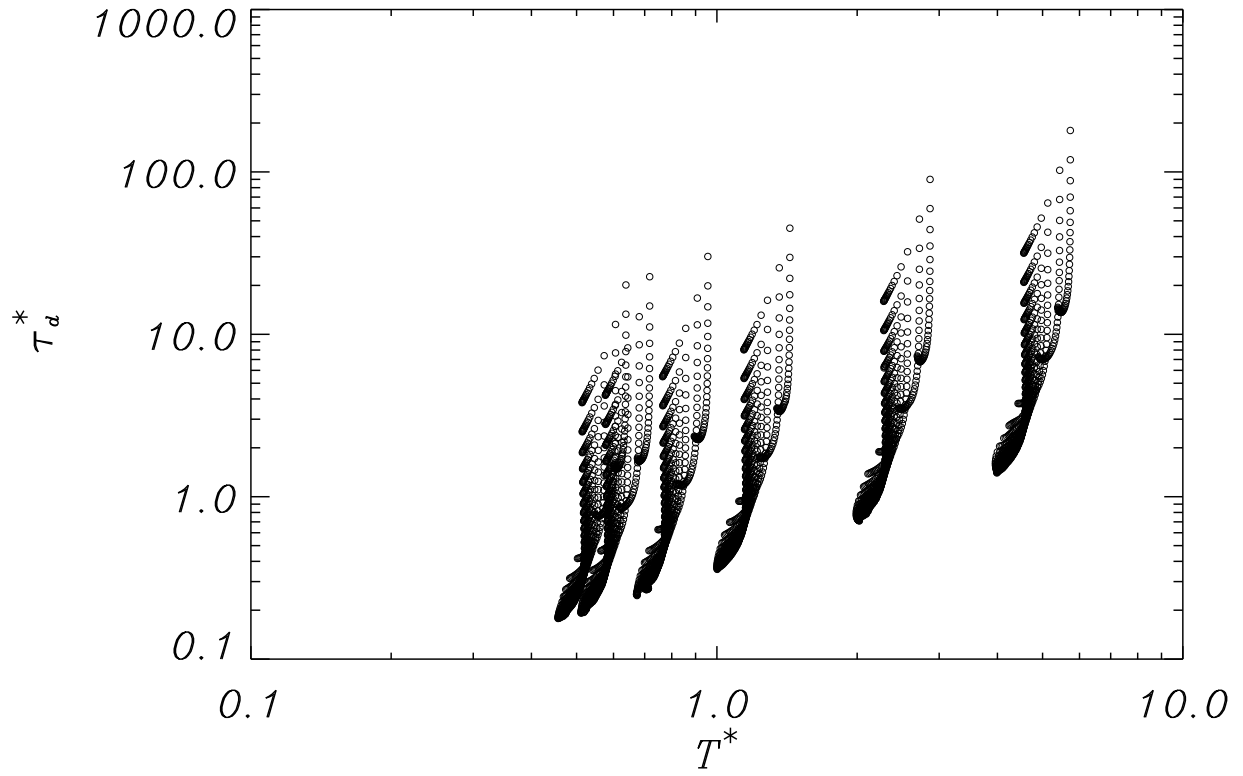


Fig. 3.— Normalized damping time as a function of the normalized period for fully non-uniform loop models with $\zeta \in [1.5, 20]$ and $l/R \in [0.1, 2]$. The six vertical strips correspond to six values of $k_z = \pi/L$.